

## **High-performance bio-inspired Composite T-joints**

Roya Akrami<sup>a</sup>

<sup>a</sup> Department of Engineering, Design and Mathematics, University of the West of England (UWE), Bristol BS16 1QY, UK

Sakineh Fotouhi<sup>b</sup>

<sup>b</sup> Department of Mechanical Engineering, University of Tabriz, Tabriz, Iran

Mohamad Fotouhi<sup>c</sup>

<sup>c</sup> University of Glasgow, School of Engineering, Glasgow G12 8QQ, UK

Mahdi Bodaghi<sup>d</sup>

<sup>d</sup> Department of Engineering, School of Science and Technology, Nottingham Trent University, Nottingham NG11 8NS, UK

Joseph Clamp<sup>a</sup>

<sup>a</sup> Department of Engineering, Design and Mathematics, University of the West of England (UWE), Bristol BS16 1QY, UK

Corresponding author

Amir Bolouri<sup>a</sup>

<sup>a</sup> Department of Engineering, Design and Mathematics, University of the West of England (UWE), Bristol BS16 1QY, UK

# High-performance bio-inspired Composite T-joints

Roya Akrami<sup>a</sup>, Sakineh Fotouhi<sup>b</sup>, Mohamad Fotouhi<sup>c</sup>, Mahdi Bodaghi<sup>d</sup>, Joseph Clamp<sup>a</sup>, Amir Bolouri<sup>a</sup>

<sup>a</sup> Department of Engineering, Design and Mathematics, University of the West of England (UWE), Bristol BS16 1QY, UK

<sup>b</sup> Department of Mechanical Engineering, University of Tabriz, Tabriz, Iran

<sup>c</sup> University of Glasgow, School of Engineering, Glasgow G12 8QQ, UK

<sup>d</sup> Department of Engineering, School of Science and Technology, Nottingham Trent University, Nottingham NG11 8NS, UK

**Abstract:** This paper introduces a novel bio-inspired design strategy based on the optimised topology of bird bone's joint to improve the strength-to-weight ratio and damage tolerance of composite T-joints. Better structuring the constituents' materials near the sharp bends results in re-distribution of stress over a larger area and reduces the stress concentration. This is done by an integrally formed support structure that is spaced apart from the main body of the T-joint in the vicinity of the bend using a Polyvinyl Chloride (PVC) foam. The support structure acts as a buttress across the bend and improves the performance of the T-joint. The T-joints are fabricated using wet layup process, from 2/2 twill TC35-carbon fibre fabric/SR5550 epoxy resin, and are subjected to quasi-static and fatigue bending, and quasi-static tensile pull-out tests. The quasi-static results reveal that the bio-inspired T-joint design has huge improvements compared to a conventional T-joint in the elastic stiffness (over 60%), peak load (over 40%) and absorbed mechanical energy (over 130%). There is only 3% weight increase in the bio-inspired T-joint compared to the conventional one. The fatigue results show a significant improvement for the bio-inspired design proving the efficiency of the novel bio-inspired design for both quasi-static and cyclic loadings.

**Keywords:** T-joint, composite, bio-inspired, bending, pull-out, fatigue.

## 1- Introduction

Joints and interfaces are one of the key aspects of the design and production of composite structures, and are often considered as the weakest links within the structure as they face high interlaminar stress concentrations and low through-thickness material strength. Conventional T or L-joints experience through-thickness (interlaminar) tensile and shear stresses that trigger progressive failure through a combination of matrix cracking and delamination [1–5].

In the FE models and experimental investigations, it has been shown that materials and geometry variations have significant influence on the stress distribution throughout T-Join and thus strongly affects the failure mode and the performance of T-joints [1-3]. For a single L-joint, it has been shown that the bend region is the critical point for failure as a result of excessive through-thickness tensile stresses, which causes delamination failure [4, 5]. These local stresses are much higher than the applied stress at the geometric stress raiser such as the radius and delta-fillet regions (Fig.1 ), where the stiffener and skin sections of the joint are connected. Consequently, the local stresses will cause concentrated damage at the regions . Hence, conservative certification requirements should be considered for safety reasons to avoid rapid brittle failure of conventional T or L-joints, partly contradicting the weight-saving benefit of composites. Different methods have been used to improve the efficiency and damage resistance of conventional T-joints including use of toughened resins [6,7], redesigning the radius/delta-fillet region to reduce the geometric stress concentration [8], and inserting through-thickness reinforcement such as stitches or z-pins [9-11].

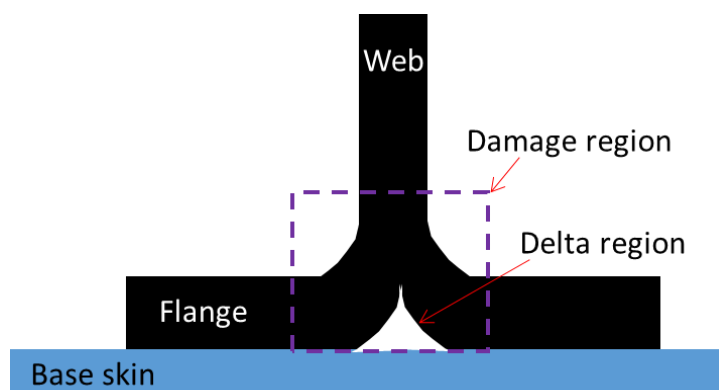


Fig. 1. A schematic of a conventional composite T-joint.

Biomimetic engineering mimics the design principles from nature and applies them to engineered materials and structures [12–15]. Biological structures such as trees or skeletal structures are self-optimised to the condition of uniform strain [16-20]. The advantage of uniform strain is that the material is distributed based on the applied stress and there are no overloaded or underloaded sites, and therefore the structural weight efficiency of the joint is maximised. There have been several studies on how a hierarchical layup of the tree branch–trunk joint can improve the performance of a composite T-joint. Based on the biological design of tree branches embedded into the centre of the trunk, Burns LA and et al. [21-23] designed bio-inspired T-joints by embedding composite plies from the flange into the skin of the carbon/epoxy T-joints. The T-joints were experimentally subjected to tension and bending loads [21]. The results showed 40% increase in maximum load and 75% increase in elastic strain absorption for the bending tests. However, this bio-inspired design reduces the stiffness in the case of tensile loading, and the damage initiates at load levels lower than the conventional design.

Another excellent design in nature is related to the extraordinary capability of feathers and bones in birds, which are extreme lightweight biological materials [24]. Hierarchically organized structures in feathers and bones enable a balance between lightweight and bending/torsional stiffness and strength. Fig. 2 illustrates examples of micro computerized tomography scans of the wing bones of the Turkey Vulture (Fig. 2a) and California Condor (Fig. 2b). The bones of these species have a thin, dense exterior with a hollow or less compact interior. Therefore material positioned further from the neutral axis is more effective in resisting bending because the stiffness is given by the product of the area moment of inertia and the material's Young's modulus [25].

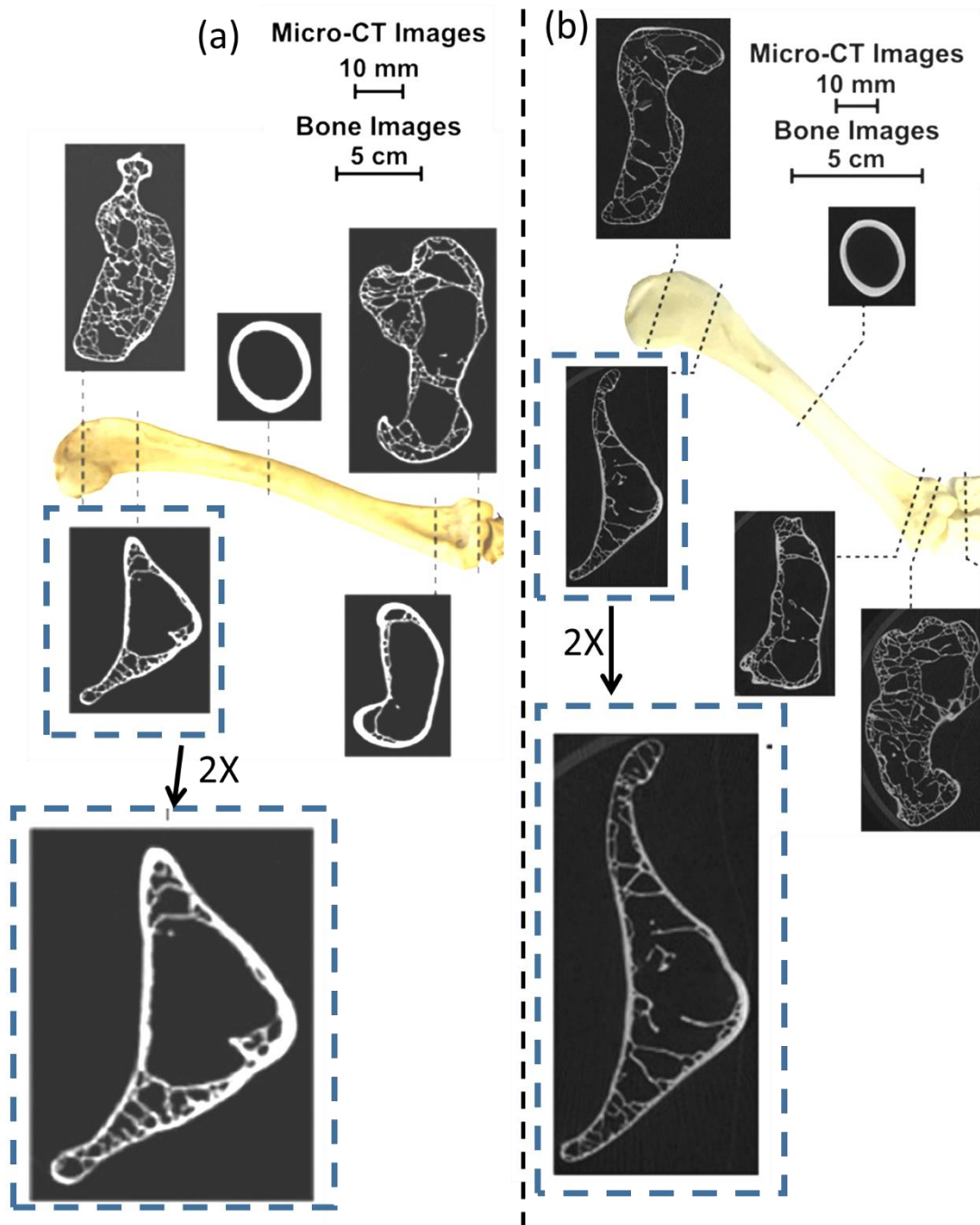


Fig. 2. Micro computerized tomography scans of the wing bones of the: (a) Turkey Vulture (*Cathartes aura*), and (b) California Condor (*Gymnogyps californianus*), pictures adapted from [24]. Zoomed parts (200%) of the joints, in the dashed rectangles, have a geometry analogous to an L-joint.

The objective of this study is to utilise the design strategies of the hollow structure of the bird's bone joints found in nature to create new design concepts for composite T-joints that are easily implementable using conventional manufacturing methods. Toward the ends of

each bone (Fig. 2), there are reinforcing structures to distribute the material based on the applied stresses throughout the bones and to counteract the stress concentration caused by the geometry of the joint. The parts in the dashed rectangles (Fig. 2) have a geometry analogous to an L-joint. The hierarchical structure of these parts is used as an inspiration for the bio-inspired design in this paper. It is worth mentioning that in this study, the design approach mainly mimics the open design with a thin membrane aspect of bird wing bones. Other biomimic scales of optimization such as cellular to structural is not a part of this study.

Fig. 3 illustrates the implementation of the bio-inspired design approach in this study to develop a novel composite T-joint in comparison with a conventional T-joint. The novel design benefits from better structuring the constituents' materials near the sharp bends and increasing the radius of the bend, resulting in re-distribution of stress over a larger area and reduces the stress concentration. This is done by integrally formed support structures (mimics the thin and dense exterior for bones in birds) that are spaced apart from the main body of the joint using a foam (mimics the hollow) in the vicinity of the bend (mimics the counteract of the stress concentration caused by the geometry). The support structure may act as a brace or buttress across the bend, in order to improve the strength of the joint around the bend. The ultimate goal is to improve the strength to weight ratio and damage tolerance of composite T-joints. Finite element analysis (FEA) and experimental testing of the bio-inspired carbon/epoxy T-joints are compared with conventional carbon/epoxy T-joints to quantify improvements in the structural properties.

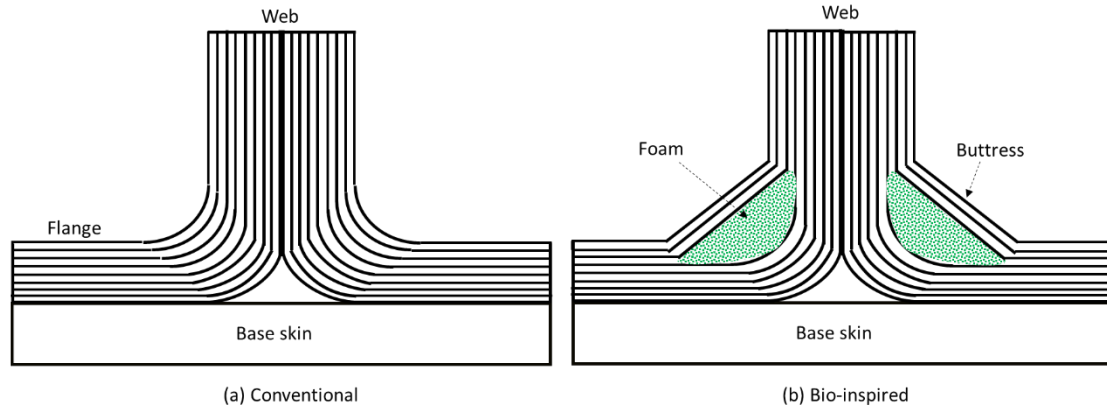


Fig. 3. Conventional T-joint design versus and the novel bio-inspired design proposed in this research work.

## 2- Experimental

### 2-1- Materials

T-joints are fabricated from a 2/2 twill, TC35-3k carbon, 200g/1m fabric, called Black Stuff Carbon Fibre available from Easy Composites. The resin being used is Sicomin SR 5550 paired with the hardener Sicomin 5503, and the foam is used as inserts is EASYCell 75 closed-cell PVC. Properties of the utilised materials are shown in Table 1.

Table 1. Properties of the utilised materials

Type	Number of Filament	Tensile strength (MPa)	Tensile modulus (GPa)	Elongation (%)	Density (g/cm <sup>3</sup> )	Filament Diameter ( $\mu$ )
TC-35 3K fibre	3 000	4 000	240	1.6	1.8	7
SR5550/SD5503 resin	-	63	2.81	3.7	1.54	-
EASYCell 75 closed cell PVC foam	-	1.89	0.075	-	0.075	-

### 2-2- Sample Layups and Configurations

As illustrated in Fig. 4, for both conventional and bio-inspired designs, the base skin consists of 10 layers of carbon with the layup  $[0/90, \pm 45, 0/90, \pm 45, 0/90]_s$ . For the standard T-joint, each side of the T-joint (L-joint) consists of 10 layers with stacking sequence of  $[0/90, \pm 45, 0/90, \pm 45, 0/90]_s$ , this is a quasi-isotropic stacking sequence that was proven to have

a good performance in T-joints [21]. For the bio-inspired design, foam corner inserts are positioned between layers 2 and 3 of the L-joints. The foam is cut to right angle triangular prism shape, with right angle sides 20mm and a radiused bottom corner as shown in Fig. 4.

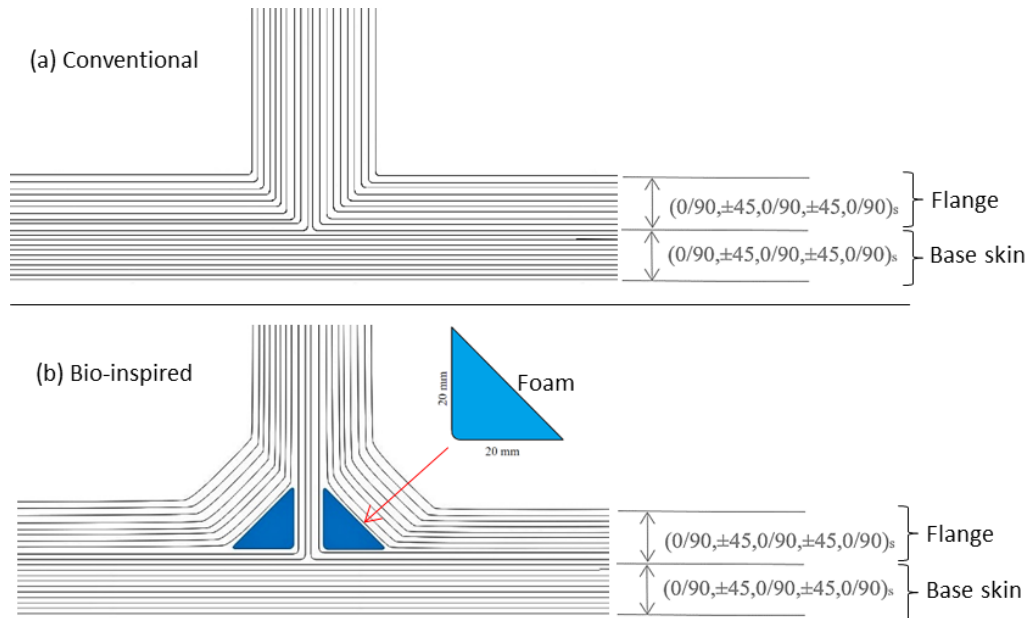


Fig. 4. Layup and configurations of the conventional and bio-inspired T-joints.

### 2-3- Manufacturing procedures

A wet layup process is used for manufacturing. The overall manufacturing procedures of the T-joints are summarised in Fig. 5. To manufacture the pairs of L-joints that are required to make each T-joint, a female mould is used. The mould has a 9mm radius and a 1.2m length that allows for the maximum number of samples to be laid up. Furthermore it speeds up production with consistency. An additional layer of peel ply fabric is laid up as the first layer in the mould, this gives the samples a pitted/rough surface finish ideal for bonding with adhesive. The fabric is weighed, and an equal measure of resin is applied in the layup. This ensures there is enough resin to fully saturate the carbon fabric. When the layup is completed a vacuum bag is applied to the mould, which applies a pressure of 1 atmosphere (1.01 Bar), ensuring full resin saturation, drawing out a percentage of the resin improving the fibre



volume fraction and preventing any gaps between the plies. For the foam core samples, the foam is inserted during the wet layup process. The base skin for all the samples is laid up as one large panel for consistency and ease of production, this is done on a large steel sheet with a peel ply surface finish and vacuum bagged to cure. Fibre volume fraction is an average of 0.50 across all panels with a standard deviation of  $\pm 0.02$ . After curing, base skin and L-joints are trimmed to slightly larger than final dimensions making them ready to be bonded into the T-joints. The bonding is performed with a slow cure Araldite 2 part epoxy for superior delamination properties. During the bonding process it is essential to apply large and consistent pressure across the entire sample on both flange/base surfaces and the web. This is achieved through the application of strong clips at regular intervals with small distances apart. Finally, when the Araldite has cured the samples are cut to size for testing. Fig. 5e and Table 2 show the dimensions and weight of the fabricated T-joints. There is about 3% increase in the weight for the bio-inspired design.

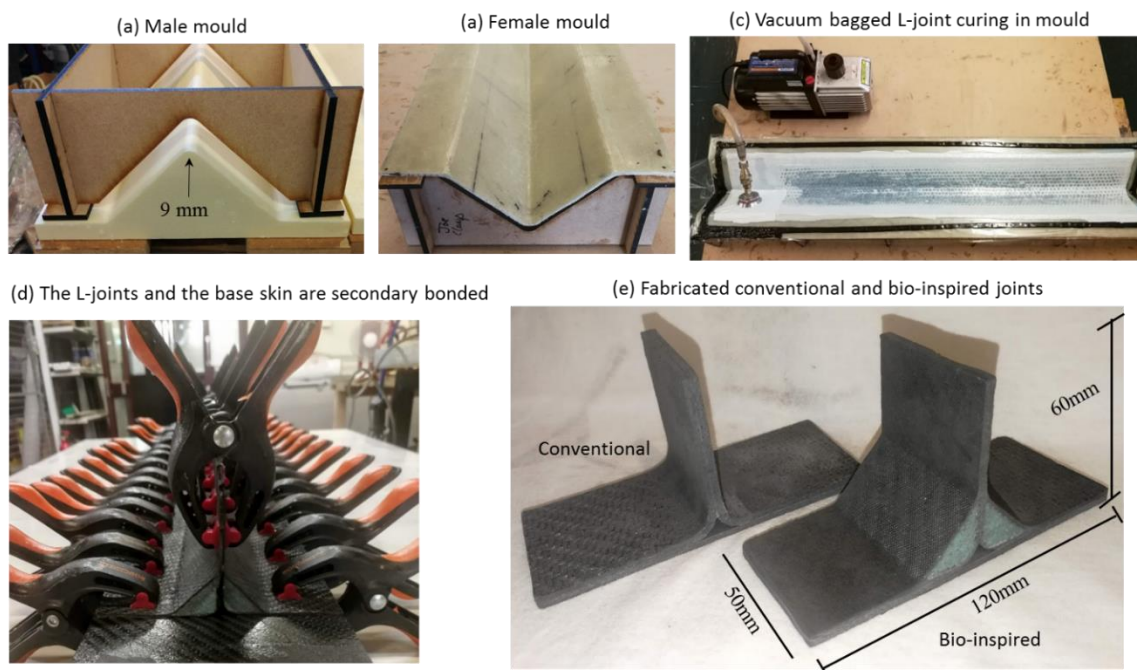


Fig. 5. The overall manufacturing procedures of the T-joints

Table 2. Average sample weight and dimensions

Type	Weight (g)	Flange thickness (mm)	Base skin thickness (mm)	Width (mm)
Conventional	58±0.5	5±0.5	5±0.5	50±0.5
Bio-inspired	60±0.5	5±0.5	5±0.5	50±0.5

#### 2-4- Mechanical Testing

As shown in Fig. 6, bending and tensile quasi-static loads are used to gather results on all of the sample variations. A minimum of three samples were tested for each case. Both tests are performed using an Instron 5982 tensile testing machine with a 100kN load cell, with the sample orientation and load direction changing. The bending tests are conducted for all samples by applying a load at a rate of 10mm/min to the web while the flange is fixed (encastre). The pull-out test is conducted by fixing the flange on a horizontal plate, and applying aluminium tabs using 24-hour cure Araldite. The flange is gripped and pulled away from the web at 5mm/min, as there is expected to be less displacement to failure than in bending so a slower feed rate is used to capture the data more accurately. The fatigue tests are performed just for the bending load. All fatigue tests are conducted under load control by applying a sinusoidal load around the mean load at a frequency of 3Hz and a tension-tension case. R-ratio for fatigue testing was 0.1.

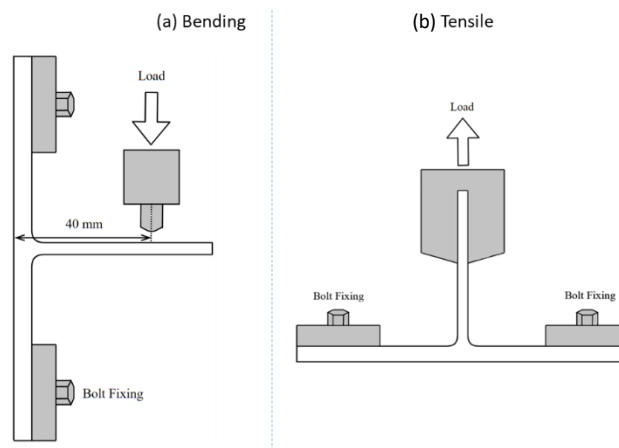


Fig. 6. Schematic and experimental setup of mechanical tests (a) bending and (b) tensile pull out.

### 3- Analysis of the bio-inspired T-joint versus a conventional T-joint

FEA using ABAQUS 6.9–2 is performed on the T-joints under bending load to give an estimate on the effectiveness of the novel bio-inspired design. Continuum shell elements of type SC8R are used for the composite parts. Controls are used to set the element shape to hex. Mesh controls are used on the resin delta region to set the elements as wedge solids of type C3D6 due to the sharp corners of this geometry. Solid C3D8R brick elements are used for the foam regions of the model. Equivalent single layer theory is used as the approach to model the composite parts. A 0.8mm mesh face size is identified a suitable mesh density by carrying out a convergence study. The input for materials property is the tensile, compression and shear strengths of a carbon/epoxy laminate in both longitudinal and transverse directions. The input data are calculated considering 50% fibre volume fraction. Some of the input properties are used from literature for similar composites. As the input values are not precise, the simulation results are not expected to be quantitatively accurate. However, an approximation on the effectiveness of the bio-inspired design should be achieved. Fig. 7 shows FEA Von Mises stress distribution and Hashin's failure criterion distribution for the T-joints. For an external bending load of 3 kN, the stress concentrations are found around the bends and resin-rich  $\Delta$ -fillet region for the conventional design. While the maximum Von Mises stress is much lower for the bio-inspired design and it is far from the bend and  $\Delta$ -fillet region. Based on Hashin's failure criterion, the failure location for the conventional T-joint is near the radii transition at the applied load level of 7kN. For the bio-inspired T-joint, the failure location is far from the bend area and happens at a higher load level of 11kN (Fig. 7). Fig. 8 compares the Von Mises stress distribution for the conventional and bio-inspired designs and it clearly can be seen that the induced stress is much lower for the bio-inspired design for an identical externally applied load. For the sake of comparison at higher loads, the stress for the conventional T-joint after failure is shown. For the conventional T-joint in

Figure 8, the initial failure of composite occurs at the load of around 3.70 kN, where a kink starts. Therefore, it can be assumed that the stress distribution is different in the damage area. Consequently, by further increasing the load to 7.00 kN, the rate of increase in stress as a function of load is lower compared to the loads before the failure. In other words, the difference between the rate of increase in the stress before and after the failure creates the kink. However, the stress after failure is not shown for the bio-inspired joint in Figure 8.

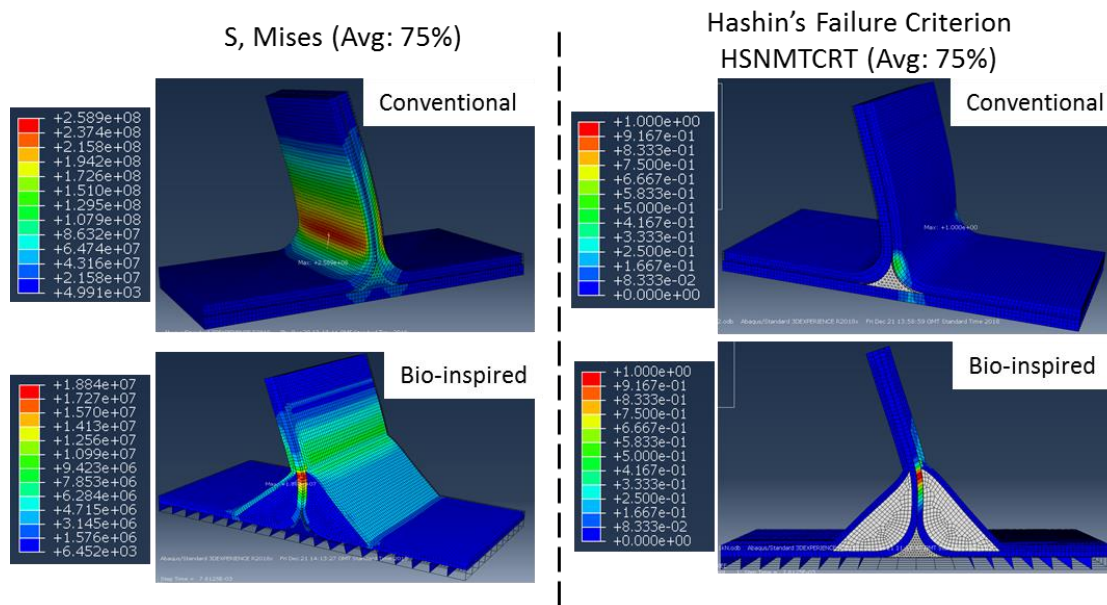


Fig. 7. FEA Von Mises Stress distribution (for 3kN applied bending load), and FEA Hashin's failure criterion (reached 1 at 7 kN for the conventional and 11 kN for the bio-inspired T-joints). For stress distribution, note the scale bar that the maximum stress (red colour) is smaller for bio-inspired joint compared to conventional one.

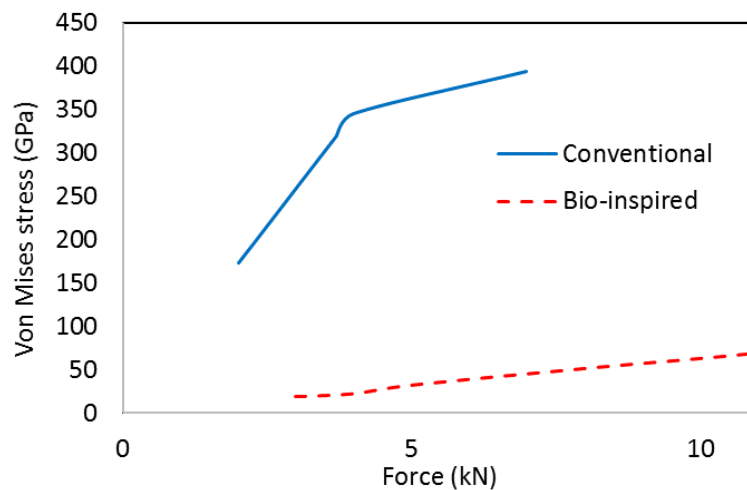


Fig. 8. Maximum Von Mises stress vs applied bending load.

#### **4- Experimental results**

##### **4-1- Quasi-static bending results**

Fig. 9 shows load-displacement curves for the T-joints subjected to the bending load. A minimum of three tests was repeated for each loading condition and design. There is a similar trend followed by each design under the identical testing condition. It should be noted that the maximum displacement is dictated by the tooling being stopped before sliding off the web not by the web breaking off. Table 3 summarises some of the key features to compare the mechanical performance of the bio-inspired and conventional designs. The damage initiation load is measured as the point at which the first load drop occurs in the linear part of the curves. Peak load is measured as the maximum load recorded within the test. Elastic stiffness is the slope of the initial linear line in the load-displacement curve. The absorbed elastic strain energy and total absorbed energy are measured as the area under the load-displacement curve up to the initial damage (first load drop) and the final failure, respectively. For the bio-inspired design, the strength to weight ratio (the peak load/weight) has 127% improvement compared the conventional design. Although the weight of bio-inspired T-joint is slightly higher by 3% compared to the conventional T-joint, the load at the initial damage and peak load are considerably higher for the bio-inspired T-joint. The load at initial fracture is increased by 1.1kN (76%) and the peak load is increased by approximately 2.2kN (134%) making the bio-inspired T-joint over 2.3 times stronger than the conventional one. The stiffness calculated from the gradient of the curve prior to initial fracture and is found to be 137% stiffer for the bio-inspired design compared with the conventional design. The bio-inspired design has 49% and 136% more energy absorption up to the initial damage and the final failure than the conventional design, respectively.

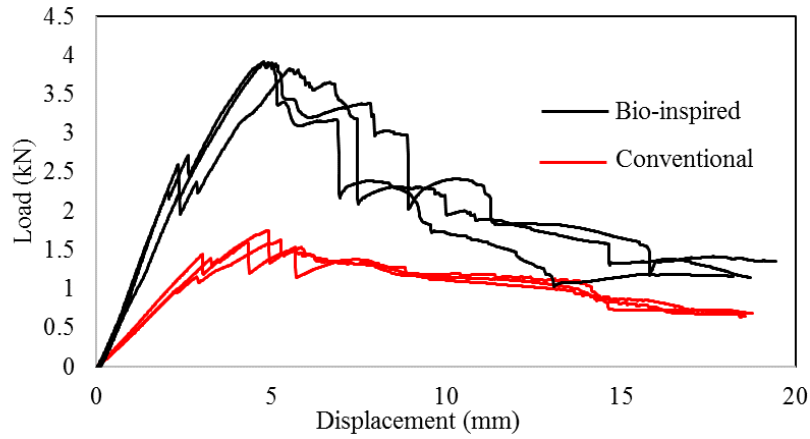


Fig. 9. Bending load-displacement curves for the investigated T-joints

Table 3. Average values for some of the key features to compare the mechanical performance of the investigated T-joints, with standard deviations given in brackets.

T-joint type	Damage initiation load (kN)	Displacement at damage initiation (mm)	Peak load (kN)	Elastic stiffness (N/mm)	Absorbed elastic strain energy (J)	Total absorbed energy (J)
Conventional	1.32±0.13	3.09±0.16	1.66±0.06	435±32	2.04±0.27	15.43±0.69
Bio-inspired	2.33±0.21	2.26±0.13	3.89±0.04	1030±70	3.08±0.38	36.49±0.66
Improvement	+76%	-26%	134%	136%	50%	136%

Fig. 10 shows typical examples of the damage in the T-joints. The images are taken after the final failure. The conventional T-joint suffers severe delamination on the radius of the obtuse side as it is straightened out in the bending motion, the small radius leads to stress concentration and consequently the damage is concentrated in that region. For the bio-inspired design, the side foam cracks are the first points of failure. The bio-inspired T-joint accumulates the damage in more areas than the conventional type, however, there is less delamination between the plies. The delamination up into the web is caused by the radius and is between far fewer layers than that in the conventional type. The fibre failure and crumpling motion occurred midway down the foam causing the crack on the side foam and lamina.

These experimental observations are in agreement with the FEA findings in the previous section regarding the damage initiation points (see Fig. 7).

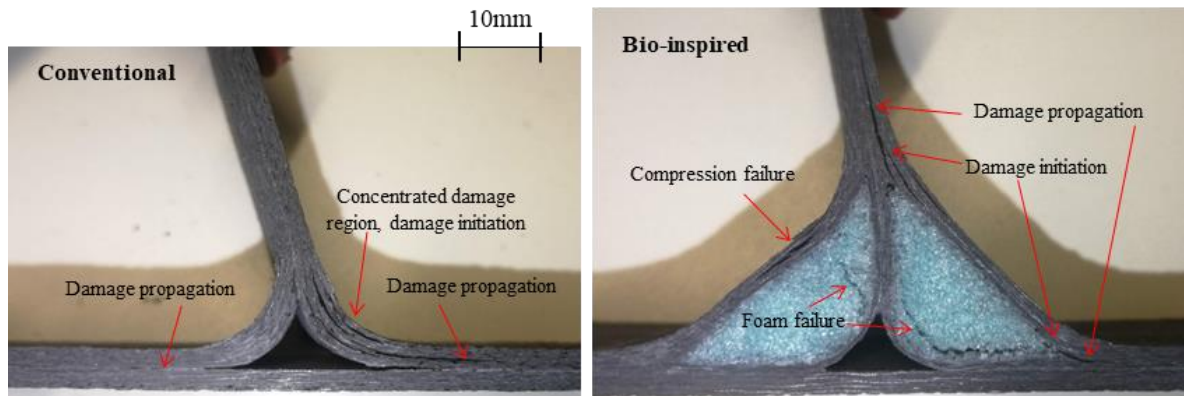


Fig. 10. Pictures are taken after the final failure under bending load from the investigated T-joints.

#### 4-2- Fatigue bending results:

Both conventional and bio-inspired T-joints are fatigued in tension-tension bending case. The maximum load levels for the fatigue tests are chosen as 75% and 90% of the damage initiation load for the conventional T-joints (i.e. 1.32kN). The loading scenario and the number of cycles before failure are given in Table 4. When sinusoidally loaded up to 75% of the damage initiation load, the conventional samples can perform approximately  $10^4$  cycles before failure. The final failure is when the T-section separates from the back. However, when the bio-inspired T-joint sample is loaded with the same sinusoidal load, it exceeded a cycle number of almost 200,000 without failure. When cycling at 90% of the damage initiation load (1.2 kN), the conventional T-joint failed just after 60 cycles, whereas the bio-inspired T-joint did not fail even after 150,000 cycles. In addition, there was no evidence for the onset of damage in bio-inspired T-joint, when the first visible damage appears.

Table 4. The bending loading scenario for the fatigue tests

T-joint type	Load range/kN	Frequency/Hz	Number of cycles before failure
Conventional-sample 1	0.07 – 0.7	3	240,000+, no failure
Conventional-sample 2	0.1 – 1.0	3	10,350
Conventional-sample 3	0.12 – 1.2	3	60
Bio-inspired-sample 1	0.1 – 1.0	3	200,000+, no failure
Bio-inspired-sample 2	0.12 – 1.2	3	150,000+, no failure

#### 4-3- Pull-out Tensile Results

Fig. 11 shows the load-displacement curves for the pull-out tensile tests performed to the investigated T-joints. Average values for some of the key features are summarised in Table 5. Some of the tensile tests are not performed to complete pull-out failure, and just one bio-inspired T-joint experienced the final pull-out. This is due to the load-cell setup, which stops the test when there is a high load drop. The conventional T-joints follow a consistent pattern with each experiencing some main load drops before the complete pull-out failure. The initial fracture varied between ~1.5kN and 2.3kN with 53% difference between them. The initial fracture of 1.5kN only causes a minor drop in the load compared to the other subsequent fractures. For bio-inspired samples, the damage initiation and peak loads are around 5.5kN and 7.2kN, which are considerably higher compared to the conventional T-joints. There is 40% improvement in strength to weight ratio (the peak load/weight) for the bio-inspired T-joint. In addition, the variation in the damage initiation loads is very small of ~5%. Table 5 shows the average key results for the pull-out tensile tests. Even though the bio-inspired samples have slightly more variation in the initial stiffness, the stiffness is higher by 168%



compared to the conventional T-joint. For the bio-inspired T-joint, the absorbed elastic strain energy and total absorbed energy have also increased by 347% and 211%, respectively. Fig. 12 shows detailed images of the damage inflicted to each T-joint. The pictures are taken just after the damage initiation, and also after the final failure. For the conventional T-joint, web delamination is the cause of initial damage followed by complete pull-out failure, where both sides of the flange have delaminated from the base section. In addition, the delamination has occurred between the two inner surfaces of the web. The bio-inspired T-joint has crack propagation in the foam leading up to delamination in the web. This is most likely due to the way the fibres are aligned, causing the plies on the outer surface of the foam to pull away from the flange. Subsequently, the crack propagates through the foam down to the web and causes delamination of the outer plies from the web. The T-section separates from the back plate in the end.

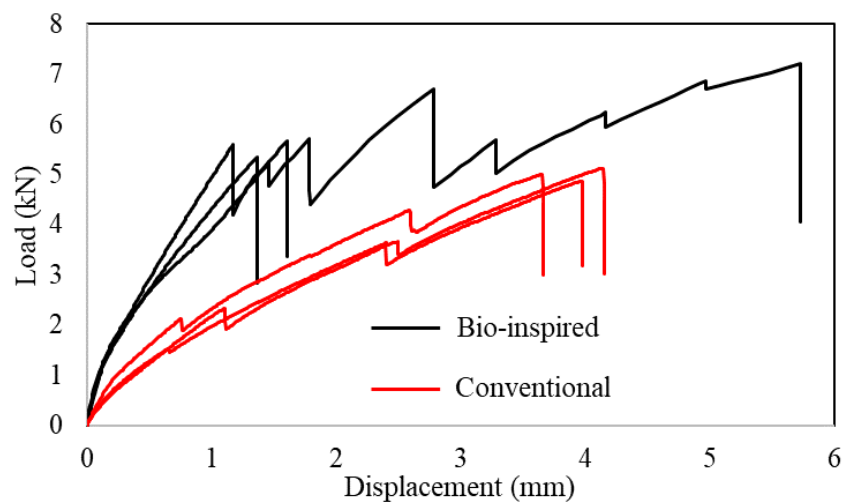


Fig. 11. Tensile load-displacement curves for the investigated T-joints

Table 5. Average values for some of the key features to compare mechanical performance of the investigated T-joints, with standard deviations given in brackets

T-joint type	Damage initiation load (kN)	Displacement at damage	Peak load (kN)	Elastic stiffness (N/mm)	Absorbed elastic	Total absorbed energy (J)

		initiation (mm)			strain energy (J)	
Conventional	1.99±0.34	0.83±0.19	5±0.10	2425±299	0.86±0.33	9.82±0.61
Bio-inspired	5.55±0.15	1.38±0.17	7.20	4081±509	3.84±0.51	30.62
Improvement	+178%	+66%	+44%	68%	346%	211%

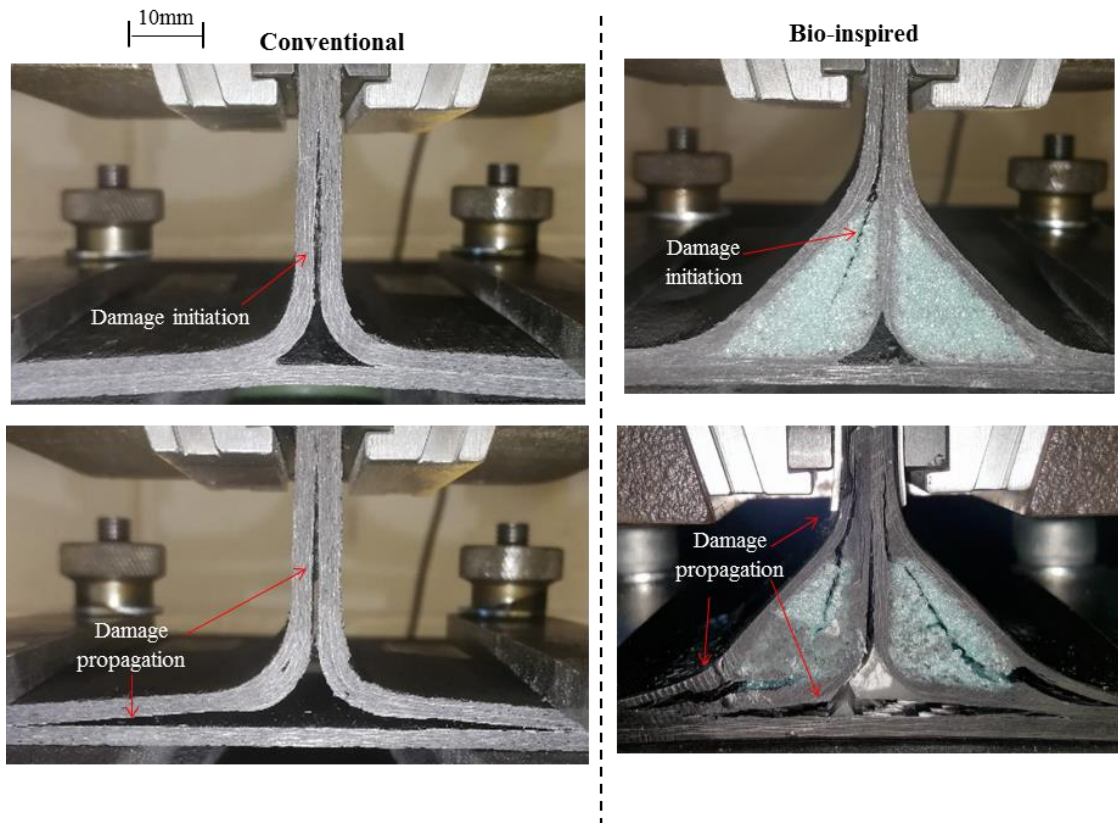


Fig. 12. Pictures are taken just after the damage initiation, and also after the final failure from the investigated T-joints, under the pull-out tensile loading.

Overall the bio-inspired design proposed in this paper has significant improvements in stiffness, strength and energy absorption for both bending and tensile loadings. The bio-inspired design has also a higher load-carrying capacity following damage initiation (damage tolerance) compared to the conventional design. These improvements are achieved with just 3% increase in the weight, and without compromising any other mechanical properties. In

addition, the design is producible using simple and inexpensive manufacturing methods such as wet layup and out of autoclave manufacturing methods.

#### **5- Future work:**

As shown in Fig. 13, composite T-joint can be optimised by combining the design principles of the tree branch–trunk joint, i.e. increasing the density of the fibres near the sharp bends and embedding composite plies from the flange into the skin, and the bone joints implemented in this paper, i.e. its hollow and hierarchical structure. Furthermore, T-joint design can be further optimised over different laminate architectures, configurations and loading conditions by investigating different locations and numbers for inserted foams, combinations of fibres (low/high modulus, short/continuous, optimised fibre characteristics), foams (shear/compression resistant foams, auxetic foams and injectable foams for self-healing and functional purposes), resins (toughened/conventional), reinforcements (toughening the critical areas using tough resins, nano particles/mats, z-pinning, mechanical interlocking and increasing local density of the fibres) and configuration parameters (shape and structure of the hierarchical design). The new designs can be optimised by finite element modelling and analytical analysis accompanied by experimental tests to obtain the desired performance. Through these designs, it can be possible to control the damage mechanisms and their location. The design principles can be expanded to I-beams, Z-beams and U-shapes.

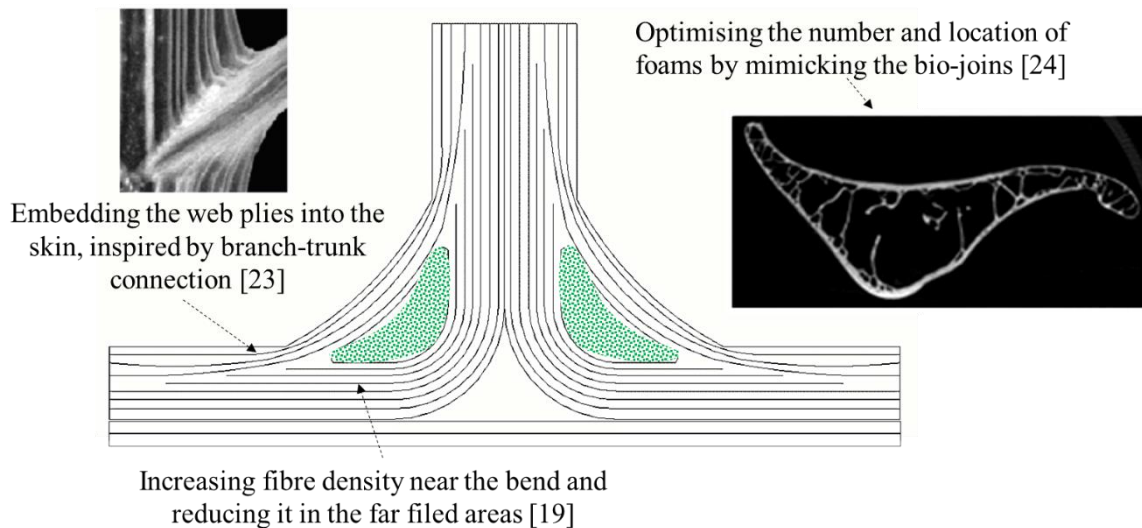


Fig. 13. Design examples for future developments of composite T-joints.

## Conclusion

This paper introduces a novel bio-inspired design strategy based on bird's bone joints to improve the strength to weight ratio and damage tolerance of composite T-joints. In the bio-inspired design the constituents' materials near the sharp bends are better structured to have a thin, dense exterior with a less compact interior to mimic the bone. Experimental testing revealed that the bio-inspired T-joint design has superior mechanical properties compared to a conventional T-joint. Huge improvement in stiffness, strength and energy absorption, are achieved using the bio-inspired design compared to a conventional joint, both in quasi-static bending and tensile pull-out tests. The bending fatigue results show a significant improvement against cyclic loading for the bio-inspired design. These improvements are achieved with only 3% weight increase, and without compromising any other mechanical properties.

## References

- [1] Orifici A, Shah S, Herszberg I, Kotler A, Weller T. Failure analysis in postbuckled composite T sections. *Compos Struct* 2008;86:146–53.

- [2] Sheno R, Hawkins G. Influence of material and geometry variations on the behaviour of bonded tee connections in FRP ships. *Composites* 1992;23(5):335–45.
- [3] Davies GAO, Hitchings D, Ankersen J. Predicting delamination and debonding in modern aerospace composite structures. *Compos Sci Technol* 2006;66(6):846–54.
- [4] Feih S, Shercliff HR. Composite failure prediction of single-L joint structures under bending. *Composites: Part A*. 2005;36:381–95.
- [5] Avalon SC, Donaldson SL. Strength of composite angle brackets with multiple geometries and nanofiber-enhanced resins. *J Compos Mater* 2010;45(9):1017–30.
- [6] Greenhalgh E, Hiley M. The assessment of novel materials and processes for the impact tolerant design of stiffened composite aerospace structures. *Composites Part A* 2003;34:151–61.
- [7] Greenhalgh E, Lewis A, Bowen R, Grassi M. Evaluation of toughening concepts at structural features in CFRP—Part I: stiffener pull-off. *Composites Part A* 2006;37:1521–35.
- [8] Mattheck C. *Design in nature: learning from trees*. New York: Springer Verlag; 1998.
- [9] Koh TM, Feih S, Mouritz AP. Experimental determination of the structural properties and strengthening mechanisms of z-pinned composite T-joints. *Compos Struct* 2011;93:2269–76.
- [10] Bianchi F, Koh TM, Zhang X, Partridge IK, Mouritz AP, Finite element modelling of z-pinned composite T-joints. *Compos Sci Technol* 2012;73:48-56.
- [11] Chen J, Ravey E, Hallett S, Wisnom M, Grassi M, Prediction of delamination in braided composite T-piece specimens. *Compos Sci Technol* 2009;69(14):2363-2367.
- [12] Chen P-Y, Lin A, Lin Y-S, Seki Y, Stokes A, Peyras J, et al. Structure and mechanical properties of selected biological materials. *J Mech Behav Biomed Mater* 2008;1:208–26.
- [13] McKittrick J, Chen P, Tombolato L, Novitskaya E, Trim M, Hirata G, et al. Energy absorbent natural materials and bioinspired design strategies: a review. *Mater Sci Eng C* 2010;30:331–42.

- [14] Espinosa H, Rim J, Barthelat F, Buehler M. Merger of structure and material in nacre and bone: perspectives on de novo biomimetic materials. *Progr Mater Sci* 2009;54:1059–100.
- [15] Meyers MA, Chen P-Y, Lin AY-M, Seki Y. Biological materials: structure and mechanical properties. *Progr Mater Sci* 2008;53:1–206.
- [16] Goetz K, Mattheck C. Trees as a model for technical fibre composites. In: Proceedings of the international conference on computer aided optimum design of structures: OPTI 2001. p. 391–400.
- [17] Reuschel D, Mattheck C. Three-dimensional fibre optimisation with computer aided internal optimisation. *Aeronaut J* 1999;103(1027):415–20.
- [18] Mattheck C, Bethge K. The structural optimisation of trees. *Naturwissenschaften* 1998;85:1–10.
- [19] Müller U, Gindl W, Jeronimidis G. Biomechanics of a branch-stem junction in softwood. *Trees* 2006;20:643–8.
- [20] Jungnikl K, Goebbels J, Burgert I, Fratz P. The role of material properties for the mechanical adaptation at branch junctions. *Trees* 2009;23:605–10.
- [21] Burns LA, Mouritz AP, Pook D, Feih S. Bio-inspired design of aerospace composite joints for improved damage tolerance. *Compos Struct* 2012; 94: 995–1004.
- [22] Burns L, Mouritz A, Pook D, Feih S. Strength improvement to composite Tjoints under bending through bio-inspired design. *Composites Part A* 2012; 43:1971–80.
- [23] Burns L, Mouritz A, Pook D, Feih S. Bio-inspired hierarchical design of composite T-joints with improved structural properties. *Composites Part B: Engineering* 2015;69: 222-231.
- [24] Sullivan TN, Wang B, Espinosa HD, Meyers MA, Extreme lightweight structures: avian feathers and bones, *Materials Today* 2017;20(7): 377-391.
- [25] Ennos R, *Solid Biomechanics*, Princeton University Press, Princeton, 2012.

